A simple and accurate generalized shear deformation theory for beams

JL Mantari[+1], J Yarasca[ϕ]

[+]Faculty of Mechanical Engineering, University of Engineering and Technology, Av. Cascanueces 2281, Santa Anita, Lima, Perú

[ϕ]Faculty of Mechanical Engineering, National University of Engineering, Av. Túpac Amaru 210, Rimac, Lima, Perú.

Abstract This paper presents a static analysis of functionally graded (FG) single and sandwich beams by using a simple and efficient 4-unknown quasi-3D hybrid type theory, which includes both shear deformation and thickness stretching effects. The governing equations and boundary conditions are derived by employing the principle of virtual works. Navier-type closed-form solution is obtained for several beams. New hybrid type shear strain shape functions for the inplane and transverse displacement were introduced in general manner to model the displacement field of beams. Numerical results of the present compact quasi-3D theory are compared with other quasi-3D higher order shear deformation theories (HSDTs).

Keywords: Beams; Elasticity; Bending, Analytical modeling.

---

[1]Corresponding Author email: jmantari@utec.edu.pe Tel: +00511 3540070; Cell: +0051 96224551;

1. Introduction

Functionally graded materials (FGMs) are a type of heterogeneous composite material in which the properties change gradually over one or more directions. FGMs made possible to avoid abrupt changes in the stress and displacement distributions. Currently, FGMs are alternative materials widely used in aerospace, nuclear reactor, energy sources, biomechanical, optical, civil, automotive, electronic, chemical, mechanical, and shipbuilding industries.

FGMs were proposed by Bever and Duwez [1], and after them several researchers have provided results on functionally graded plates [2-10], sandwich plates [11, 12], shells [13, 14] and beams [15-17]; this short list gives an idea of some contribuition in the field. Carrera et al. [18] investigated the influence of the stretching effect on the static responses of functionally graded (FG) plates and shells, which is especially significant for thick FG plates. Consequently, thickness stretching effects is also necessary to include in beam formulations for the precise mechanical prediction of stresses.

As far as the authors are aware, there is limited work available for bending analysis of FG sandwich beams. Vo et al. [19] develop a quasi-3D polynomial theory with 4 unknowns to investigate the static behaviour and the effect of normal strain in FG sandwich beams for various power-law index, skin-core-skin thickness ratios and boundary conditions. In this context, the influence of non-polynomial or hybrid type shear strain shape functions were not explored to study FG beams along with C^1 HSDTs. However, it is remarkable to mention the work by Filippi et al. [20] based on Giunta et al. [15-17] beam formulation (1D Carrera's unified formulation), where trigonometric, polynomial, exponential and miscellaneous expansions are used and evaluated for various structural problems. This paper attempts to cover this gap.

In this paper, a 4-unknown hybrid type quasi-3D theory with both shear deformation and thickness stretching effects for the bending analysis of FG beams is presented. Many quasi-3D hybrid type (polynomial, non-polynomial, and hybrid) HSDTs, including the thickness expansion can be derived by using the present generalized theory. The theory complies with the tangential stress-free boundary conditions on the beam boundary surface, and thus a shear correction factor is not required. The beam governing equations and its boundary conditions are derived by employing the principle of virtual works. Navier-type analytical solution is obtained for sandwich beams subjected to transverse load for simply supported boundary conditions. The results are compared with other quasi-3D HSDT and further referential results for the displacement and stresses of FG sandwich beams are obtained.

2. Analytical modeling of FG beams

An FG beam of length a, width b and a total thickness h made of a mixture of metal and ceramic materials are considered in the present analysis. The elastic material properties vary through the thickness and the power-law distribution [19]:

$$E(z) = (E_c - E_m)V_c(z) + E_m \tag{1}$$

where subscripts m and c represent the metallic and ceramic constituents, V_c is the volume fraction of the ceramic phase of the beam. For comparison reasons, three types of FG beams are considered, see Fig. 1.

2.1 Type A FG beams

The beam is composed of a FG material (Fig. 1a) with V_c given by:

$$V_c(z) = \left(\frac{2z+h}{2h}\right)^p \tag{2}$$

2.2 Type B sandwich beams with homogeneous skins and FG core

The bottom and top skin of sandwich beams is metal and ceramic, while, the core is composed of a FG material (Fig. 1b) with V_c given by [19]:

$$\begin{aligned} V_c &= 0 && z \in [-h/2, h_1] && \text{(bottom skin)} \\ V_c &= \left(\frac{z-h_1}{h_2-h_1}\right)^p && z \in [h_1, h_2] && \text{(core)} \\ V_c &= 1 && z \in [h_2, h/2] && \text{(top skin)} \end{aligned} \tag{3}$$

2.3 Type C sandwich beams with FG skins and ceramic core

The bottom and top skin of sandwich beams is composed of a FG material , while, the core is ceramic (Fig. 1c) with V_c given by [19]:

$$\begin{aligned} V_c &= \left(\frac{z-h_0}{h_1-h_0}\right)^p && z \in [-h/2, h_1] && \text{(bottom skin)} \\ V_c &= 1 && z \in [h_1, h_2] && \text{(core)} \\ V_c &= \left(\frac{z-h_3}{h_2-h_3}\right)^p && z \in [h_2, h/2] && \text{(top skin)} \end{aligned} \tag{4}$$

2.4. Theoretical displacement field

The displacement field satisfying the free surfaces boundary conditions of transverse shear stresses (and hence strains) vanishing at a point (x, $\pm h/2$) on the outer (top) and inner (bottom) surfaces of the beam, is given as follows:

$$\begin{aligned} \bar{u}(x,z) &= u + z\left[y^{**}\frac{\partial w_b}{\partial x} + q^{*}\frac{\partial \theta}{\partial x} - \frac{\partial w_s}{\partial x} \right] + f(z)\frac{\partial w_b}{\partial x} \\ \bar{w}(x,z) &= w_b + w_s + g(z)\theta \end{aligned} \tag{5}$$

where u , w_s , w_b and θ are four unknown displacements of midplane of the beam. The constants y^{**} , y^{*} and q^{*} are obtained by considering the criteria to reduce the number of unknowns in HSDTs as in Reddy and Liu [21]. They are as a function of the shear strain shape functions, $f(z)$ and $g(z)$, i.e. $y^{**} = y^{*} - 1$, $y^{*} = -f'(\frac{h}{2})$ and $q^{*} = -g(\frac{h}{2})$.

For deriving the equations, small elastic deformations are assumed, i.e. displacements and rotations are small, and obey Hookes law. The starting point of the present generalized quasi-3D HSDT is the 3D elasticity theory [22]. The strain-displacement relations, based on this formulation, are written as follows:

$$\begin{aligned} \varepsilon_{xx} &= \varepsilon_{xx}^{0} + z\varepsilon_{xx}^{1} + f(z)\varepsilon_{xx}^{2} \\ \varepsilon_{zz} &= g'(z)\varepsilon_{zz}^{5} \\ \gamma_{xz} &= \gamma_{xz}^{0} + g(z)\gamma_{xx}^{3} + f'(z)\gamma_{xz}^{4} \end{aligned} \tag{6}$$

where

$$\begin{aligned} &\varepsilon_{xx}^{0} = \frac{\partial u}{\partial x} && \varepsilon_{xx}^{1} = y^{**}\frac{\partial^2 w_b}{\partial x^2} + q^{*}\frac{\partial^2 \theta}{\partial x2} - \frac{\partial^2 w_s}{\partial x^2} && \varepsilon_{xx}^{2} = \frac{\partial^2 w_b}{\partial x^2} \\ &\varepsilon_{zz}^{5} = \theta && && \\ &\varepsilon_{xz}^{0} = y^{*}\frac{\partial w_b}{\partial x} + q^{*}\frac{\partial \theta}{\partial x} && \varepsilon_{xz}^{3} = \frac{\partial \theta}{\partial x} && \varepsilon_{xz}^{4} = \frac{\partial w_b}{\partial x} \end{aligned} \tag{7}$$

The linear constitutive relations are given below:

$$\begin{Bmatrix} \sigma_{xx} \\ \sigma_{zz} \\ \tau_{xz} \end{Bmatrix}_{(z)} = \begin{bmatrix} Q_{11} & Q_{13} & 0 \\ Q_{13} & Q_{33} & 0 \\ 0 & 0 & Q_{55} \end{bmatrix}_{(z)} \begin{Bmatrix} \varepsilon_{xx} \\ \varepsilon_{zz} \\ \gamma_{xz} \end{Bmatrix}_{(z)} \tag{8}$$

in which, $\sigma_{(z)} = \{\sigma_{xx}, \sigma_{zz}, \tau_{xz}\}^T$ and $\varepsilon_{(z)} = \{\varepsilon_{xx}, \varepsilon_{zz}, \gamma_{xz}\}^T$ are the stresses and the strain vectors with respect to the beam coordinate system. The Q_{ij} expressions are given below:

$$\begin{aligned} Q_{11(z)} &= Q_{33(z)} = \frac{E(z)}{1-\nu^2} \\ Q_{13(z)} &= \frac{E(z)\nu}{1-\nu^2} \\ Q_{55(z)} &= \frac{E(z)}{2(1+\nu)} \end{aligned} \tag{9}$$

The elastic coefficients Q_{ij} vary through the thickness according to Eq. 1.

Considering the static version of the principle of virtual work, the following expressions can be obtained:

$$0 = [\int_{-h/2}^{h/2}\{\int_{\Omega}[\sigma_{xx}\delta\varepsilon_{xx} + \sigma_{zz}\delta\varepsilon_{zz} + \tau_{xz}\delta\gamma_{xz}]dxdy\}dz] - [\int_{\Omega} q\delta\overline{w}dxdy], \tag{10}$$

$$0 = \int_{\Omega}(N_1\delta\varepsilon_{xx}^0 + M_1\delta\varepsilon_{xx}^1 + P_1\delta\varepsilon_{xx}^2 + R_3\delta\varepsilon_{zz}^5 + N_5\delta\varepsilon_{xz}^0 + Q_5\delta\varepsilon_{xz}^3 + K_5\delta\varepsilon_{xz}^4 - q\delta\overline{w})dxdy, \tag{11}$$

where σ or ε are the stresses and the strain vectors, q is the distributed transverse load; and N_i, M_i, P_i, Q_i, K_i and R_i are the resultants of the following integrations:

$$\begin{aligned} (N_i, M_i, P_i) &= \sum_{k=1}^{N}\int_{z(k-1)}^{z^k}\sigma_i(1, z, f(z))dz, \quad (i=1), \\ N_i &= \sum_{k=1}^{N}\int_{z(k-1)}^{z^k}\sigma_i\, dz, \quad (i=5), \\ (Q_i, K_i) &= \sum_{k=1}^{N}\int_{z(k-1)}^{z^k}\sigma_i(g(z), f'(z))dz, \quad (i=5), \\ R_i &= \sum_{k=1}^{N}\int_{z(k-1)}^{z^k}\sigma_i\, g'(z)dz, \quad (i=3), \end{aligned} \tag{12}$$

where k represent a single-layer in the case of functionally graded sandwich beam.

The static version of the governing equations are derived from Eq. 11 by integrating the displacement gradients by parts and setting the coefficients of $\delta u, \delta w_b, \delta w_s$ and $\delta\theta$ to zero separately. The equations obtained are as follows:

$$\begin{aligned}
&\delta u: \quad \frac{\partial N_1}{\partial x} = 0, \\
&\delta w_b: \quad y^{**}\frac{\partial^2 M_1}{\partial x^2} + \frac{\partial^2 P_1}{\partial x^2} - y^{*}\frac{\partial N_5}{\partial x} - \frac{\partial K_5}{\partial x} = q, \\
&\delta w_s: \quad -\frac{\partial^2 M_1}{\partial x^2} = q, \\
&\delta\theta: \quad q^{*}\frac{\partial^2 M_1}{\partial x^2} + R_3 - q^{*}\frac{\partial N_5}{\partial x} - \frac{\partial Q_5}{\partial x} = -q^{*}q,
\end{aligned} \tag{13}$$

By substituting the stress–strain relations into the definitions of force and moment resultants (Eq. 12), the following constitutive equations are obtained:

$$\begin{aligned}
&N_i = A_{ij}\varepsilon_j^0 + B_{ij}\varepsilon_j^1 + C_{ij}\varepsilon_j^2 + D_{ij}\varepsilon_j^3 + E_{ij}\varepsilon_j^4 + F_{ij}\varepsilon_j^5 \quad (i=1,3);(j=1-3) \\
&M_i = B_{ij}\varepsilon_j^0 + G_{ij}\varepsilon_j^1 + H_{ij}\varepsilon_j^2 + I_{ij}\varepsilon_j^3 + J_{ij}\varepsilon_j^4 + K'_{ij}\varepsilon_j^5 \quad (i=1);(j=1-3) \\
&P_i = C_{ij}\varepsilon_j^0 + H_{ij}\varepsilon_j^1 + L_{ij}\varepsilon_j^2 + M'_{ij}\varepsilon_j^3 + N'_{ij}\varepsilon_j^4 + O_{ij}\varepsilon_j^5 \quad (i=1);(j=1-3) \\
&Q_i = D_{ij}\varepsilon_j^0 + I_{ij}\varepsilon_j^1 + M'_{ij}\varepsilon_j^2 + P'ij\varepsilon_j^3 + Q'_{ij}\varepsilon_j^4 + R'_{ij}\varepsilon_j^5 \quad (i=3);(j=1-3) \\
&K_i = E_{ij}\varepsilon_j^0 + J_{ij}\varepsilon_j^1 + N'_{ij}\varepsilon_j^2 + Q'_{ij}\varepsilon_j^3 + S_{ij}\varepsilon_j^4 + T_{ij}\varepsilon_j^5 \quad (i=3);(j=1-3) \\
&R_i = F_{ij}\varepsilon_j^0 + K'_{ij}\varepsilon_j^1 + O_{ij}\varepsilon_j^2 + R'_{ij}\varepsilon_j^3 + T_{ij}\varepsilon_j^4 + U_{ij}\varepsilon_j^5 \quad (i=2);(j=1-3)
\end{aligned} \tag{14}$$

where:

$$\begin{aligned}
&(A_{ij}, B_{ij}, C_{ij}, D_{ij}, E_{ij}, F_{ij}) = \int_{-h/2}^{h/2} Q_{ij}^{(k)}(1, z, f(z), g(z), f'(z), g'(z))dz, \\
&(G_{ij}, H_{ij}, I_{ij}, J_{ij}, K_{ij}) = \int_{-h/2}^{h/2} Q_{ij}^{(k)}(z^2, zf(z), zg(z), zf'(z), zg'(z))dz, \\
&(L_{ij}, M'_{ij}, N'_{ij}, O_{ij}) = \int_{-h/2}^{h/2} Q_{ij}^{(k)}(f^2(z), f(z)g(z), f(z)f'(z), f(z)g'(z))dz, \\
&(P'_{ij}, Q'_{ij}, R'_{ij}) = \int_{-h/2}^{h/2} Q_{ij}^{(k)}(g^2(z), g(z)f'(z), g(z)g'(z))dz, \\
&(S_{ij}, T_{ij}) = \int_{-h/2}^{h/2} Q_{ij}^{(k)}(f'^2(z), f'(z)g'(z))dz, \\
&U_{ij} = \int_{-h/2}^{h/2} Q_{ij}^{(k)} g'^2(z)dz,
\end{aligned} \tag{15}$$

The natural boundary conditions are of the form:

$$\begin{aligned}
&\delta u: \quad N_1 \\
&\delta w_b: \quad N_5 + K_5 - \frac{\partial M_1}{\partial x} - \frac{\partial P_1}{\partial x} \\
&\delta w'_b: \quad M_1 + P_1 \\
&\delta w_s: \quad \frac{\partial M_1}{\partial x} \\
&\delta w'_s: \quad -M_1 \\
&\delta\theta: \quad N_5 + Q_5 - \frac{\partial M_1}{\partial x} \\
&\delta\theta': \quad M_1
\end{aligned} \tag{16}$$

3. Solution procedure

For simply-supported boundary conditions, the Navier solution is assumed to be of the form:

$$\begin{aligned} u(x) &= \sum_{n}^{\infty} U_n \cos(\alpha x) \\ w_b(x) &= \sum_{n}^{\infty} W_{bn} \sin(\alpha x) \\ w_s(x) &= \sum_{n}^{\infty} W_{sn} \sin(\alpha x) \\ \theta(x) &= \sum_{n}^{\infty} \Theta_n \sin(\alpha x) \end{aligned} \tag{17}$$

where

$$\alpha = n\pi / L, \tag{18}$$

From Eq. 14, it can be noticed that for $N_i, M_i, P_i, Q_i, K_i,$ and R_i, the variables depending on x are the generalized strains, ε_j^b (b = 0,...,5). Therefore, the expressions in each of the beam governing Eqs. 13, for example $\frac{\partial^2 N_i}{\partial x^2}$, $\frac{\partial^2 M_i}{\partial x^2}$, can be expressed as follows:

$$\frac{\partial^2 (N_i, M_i)}{\partial x^2} = (A_{ij}, B_{ij}) \left[\begin{bmatrix} \alpha^3 & 0 & 0 & 0 \\ 0 & 0 & 0 & 0 \\ 0 & -y^* \alpha^3 & 0 & -q^* \alpha^3 \end{bmatrix} \begin{Bmatrix} U_n \\ W_{bn} \\ W_{sn} \\ \Theta_n \end{Bmatrix} \right]^T \times \begin{Bmatrix} S \\ S \\ C \end{Bmatrix} +$$

$$(B_{ij}, G_{ij}) \left[\begin{bmatrix} 0 & y^{**} \alpha^4 & -\alpha^4 & q^* \alpha^4 \\ 0 & 0 & 0 & 0 \\ 0 & 0 & 0 & 0 \end{bmatrix} \begin{Bmatrix} U_n \\ W_{bn} \\ W_{sn} \\ \Theta_n \end{Bmatrix} \right]^T \times \begin{Bmatrix} S \\ S \\ C \end{Bmatrix} +$$

$$(C_{ij}, H_{ij}) \left[\begin{bmatrix} 0 & \alpha^4 & 0 & 0 \\ 0 & 0 & 0 & 0 \\ 0 & 0 & 0 & 0 \end{bmatrix} \begin{Bmatrix} U_n \\ W_{bn} \\ W_{sn} \\ \Theta_n \end{Bmatrix} \right]^T \times \begin{Bmatrix} S \\ S \\ C \end{Bmatrix} +$$

$$(D_{ij}, I_{ij})\left[\begin{bmatrix} 0 & 0 & 0 & 0 \\ 0 & 0 & 0 & 0 \\ 0 & 0 & 0 & -\alpha^3 \end{bmatrix}\begin{Bmatrix} U_n \\ W_{bn} \\ W_{sn} \\ \Theta_n \end{Bmatrix}\right]^T \times \begin{Bmatrix} S \\ S \\ C \end{Bmatrix} + \tag{19}$$

$$(E_{ij}, J_{ij})\left[\begin{bmatrix} 0 & 0 & 0 & 0 \\ 0 & 0 & 0 & 0 \\ 0 & -\alpha^3 & 0 & 0 \end{bmatrix}\begin{Bmatrix} U_n \\ W_{bn} \\ W_{sn} \\ \Theta_n \end{Bmatrix}\right]^T \times \begin{Bmatrix} S \\ S \\ C \end{Bmatrix} +$$

$$(F_{ij}, K_{ij})\left[\begin{bmatrix} 0 & 0 & 0 & 0 \\ 0 & 0 & 0 & -\alpha^2 \\ 0 & 0 & 0 & 0 \end{bmatrix}\begin{Bmatrix} U_n \\ W_{bn} \\ W_{sn} \\ \Theta_n \end{Bmatrix}\right]^T \times \begin{Bmatrix} S \\ S \\ C \end{Bmatrix},$$

where S = sin(α x), C = cos(α x) and so for, and the elements of the 3×4 matrices are the coefficients obtained after taking the second derivation of the strain expressions in Eq. 14. As is known, the strains are expressed as a function of the 4 unknowns, described in Eq. 5 and Eq. 17.

The 3×4 matrices associated with $\dfrac{\partial^2 (N_i, M_i)}{\partial x^2}$ in Eq. 19, is called $\overline{M}_x^{(2,b)}$ (b = 0,...,5). The symbols used in $\overline{M}_v^{(a,b)}$ are as follow: the first upper and lower (a, v) indicates the derivative (second derivative with respect to *x*, in the example), and the second upper character, b, indicates that the derivative is associates with the strain ε_j^b (b = 0,..., 5). Therefore, the expression $\dfrac{\partial^2 (N_i, M_i)}{\partial x^2}$, can be expressed as:

$$\begin{aligned}\frac{\partial^2 (N_i, M_i)}{\partial x^2} = \quad & (A_{ij}, B_{ij})\overline{M}_x^{2,0} + (B_{ij}, G_{ij})\overline{M}_x^{2,1} + (C_{ij}, H_{ij})\overline{M}_x^{2,2} \\ & + (D_{ij}, I_{ij})\overline{M}_x^{2,3} + (E_{ij}, J_{ij})\overline{M}_x^{2,4} + (F_{ij}, K_{ij})\overline{M}_x^{2,5},\end{aligned} \tag{20}$$

where, for example, $\overline{M}_x^{2,0}$ is:

$$\overline{M}_x^{2,0} = \begin{bmatrix} \alpha^3 & 0 & 0 & 0 \\ 0 & 0 & 0 & 0 \\ 0 & -y^*\alpha^3 & 0 & -q^*\alpha^3 \end{bmatrix}, \tag{21}$$

All matrices of type, $\overline{M}_v^{(a,b)}$, associated with the expressions of the beam governing Eqs. 13, for example $\frac{\partial N_i}{\partial x}$ or $\frac{\partial^2 M_i}{\partial x^2}$, are given in Appendix A.

In summary, substituting Eq. 17 into Eq. 13 by following the procedure described above, the following equations are obtained,

$$K_{ij} d_j = F_i \quad (i, j = 1,....,4) \quad \text{and} \quad (K_{ij} = K_{ji}) \tag{22a}$$

Elements of K_{ij} in Eq. 22a can be obtained by using the matrices $\overline{\mathrm{M}}_{\mathrm{v}}^{(\mathrm{a,b})}$, and the governing Eqs. 13.

$$\{d_j\}^T = \{U_n, W_{bn}, W_{sn}, \Theta_n\}^T \tag{22b}$$

$$\{F_j\}^T = \{0, Q_n, Q_n, -q^* Q_n\}^T \tag{22c}$$

where Q_n are the coefficients in the Fourier expansion of the uniform load (q_o),

$$q(x) = \sum_n^{\infty} Q_n sin(\alpha x) = \sum_n^{\infty} \frac{4q_o}{m\pi} sin(\alpha x) \quad with \quad n = 1,3,5... \tag{23}$$

3. Numerical Results

The results of the present hybrid type quasi-3D HSDT with 4-unknowns contemplates the recommendations regarding the stretching effect (see Ref. [18]). The target of this paper is present: (a) the generalized mathematical formulation for the quasi-3D HSDT with 4 unknowns; and (b) present the results of using polynomial, non-polynomial and quasi-3D hybrid type HSDTs for various FG sandwich beams.

It was not the intent of this paper to present the best quasi-3D HSDT having 4-unknowns. However, so far very accurate quasi-3D HSDT with 4 unknowns can be obtained by just using referential shear strain shape functions developed previously by the authors [7, 19].

Table 1 presents different couples of shear strain shape functions to be evaluated in the present quasi-3D HSDT with 4-unknowns. The first quasi-3D HSDT is a polynomial HSDT, the second HSDT is the well-known trigonometric quasi-3D HSDT, the third one is a resent trigonometric quasi-3D HSDT propose by Mantari and Guedes Soares [7], and the last one is a hybrid type (which combines polynomial with non-polynomial shape strain functions and vice versa, respectively), i.e. quasi-3D hybrid type HSDTs. For simplicity, the theories are called HSDT1, HSDT2 and so for (see Table 1). In case of the present quasi-3D hybrid type HSDT (HSDT4) it is important to properly select the shears strain function in order to get accurate results. However, for some hybrid shear strain functions such as exponential and trigonometric, this is not easy task. This is alleviated when one of the hybrid shears strain function is polynomial as in HSDT4 (see Mantari and Guedes Soares [7]).

Navier solution is used to validate the bending behaviour of FG sandwich beams under an uniformly distributed load *q*. Displacements and stresses of symmetric and non-symmetric sandwich beams with FG material in the core or skins are calculated. Various power-law indexes and skin-core-skin thickness ratios are considered. FG sandwich beams made of Aluminum as metal (Al: $E_m = 70$ GPa, $\nu_m = 0.3$) and Alumina as ceramic (Al_2O_3: $E_c = 380$ GPa, $\nu_m = 0.3$) with two slenderness ratios, a/h equal to 5 and 20, are considered. For convenience, the following non-dimensional terms are used:

$$w = \frac{100E_m h^3}{qa^4} w(\frac{a}{2}, z), \tag{24a}$$

$$\bar{\sigma}_{xx} = \frac{h}{qa}\sigma_{xx}(\frac{a}{2}, z) \tag{24b}$$

$$\bar{\sigma}_{zz} = \frac{h}{qa}\sigma_{zz}(\frac{a}{2}, z) \tag{24c}$$

$$\bar{\sigma}_{xz} = \frac{h}{qa}\sigma_{xz}(0, z) \tag{24d}$$

3.1 Type A: FG beams

FG beams (Type A) under an uniformly distributed load are considered. The maximum displacements and stresses obtained from the different HSDTs are given in Tables 2 to 5 along with the results from previous referential studies (Ref. [19]). Table 2 presents results of non-dimensionalized maximum beam deflections, it is clear that the results agree completely with Ref. [19]. From Table 4 can be noticed that HSDT3 results do not agree with the others for higher values of *p*, this may be due to the fact that the functions $f(z)$ and $g(z)$ are not ideal for this case or need to be carefully optimized for this kind of application. Even so, Fig. 2 shows strong similarities in results with Ref. [19]. Therefore, all the HSDTs presented in this paper are acceptable.

3.2 Type B: Sandwich beams with homogeneous skins FG core

In this example, bending analysis of (1-8-1) sandwich beams of Type B is performed. The results are given in Tables 6 to 9. From Tables 6 and 7 can be noticed the sligth influence of the selected shear strain shape function *f(z)* in the displacements and stresses results for HSDT3 and HSDT4. In Table 8 can be seen that as the value of p increases, for $a/h = 5$, HSDT2, HSDT3 and HSDT4 produces different results than HSDT1 and Ref. [19]. Fig. 3 shows the maximum values of axial, normal and shear stresses for different power-law index using the HSDT4. Maximum tensile axial stress and the maximum shear stress is obtained for $p = 10$ at the top (ceramic-rich) surface and the top surface of core layer respectively as in Ref. [19]. However, the maximum normal stress is obtained at the bottom surface for $p = 5$.

3.3 Type C: Sandwich beams with FG skins ceramic core

Finally, two types of symmetric (1-2-1) and non-symmetric (2-2-1) sandwich beams of Type C are considered. The vertical displacement and stresses for various HSDTs are given in Tables 10 to 13. Again HSDT3 differs from the others results as p increases for the two normal stresses, σ_{xx} and σ_{zz}. Fig. 4 shows the vertical displacements along the thickness for different p values. There are some difference between symmetric and non-symmetric beams. For the symmetric beam (Figs. 5a and

6a), the maximum tensile (compressive) axial and normal stress are at the top (bottom) surface of the core layer. However, for non-symmetric ones (Figs. 5b and 6b), the maximum tensile axial stress occurs at the top surface of core layer and while the maximum compressive normal stress occurs at the bottom surface of core layer. Fig 7 shows that the maximum shear stress for both symmetric and non-symmetric beams occurs at the midplane of the beam.

4. Conclusions

A generalized hybrid type quasi-3D HSDT with only 4-unknowns and stretching effects to study advanced composite beams is presented in this paper. The governing equations and boundary conditions are derived by employing the principle of virtual work. A Navier-type closed-form solution is obtained for functionally graded single and sandwich beams subjected to distribuited load for simply supported boundary conditions. The important conclusions that emerge from this paper can be summarized as follows:

a) Multiple shears strain shape function can be evaluated by using the present theory.
b) So far polynomial shear strain functions are easy to implement and simple to compute. In this type of case studies the present polynomial quasi-3D HSDT produce very accurate results.
c) Hybrid type (polynomial and non-polynomial) shear strain function are more accurate than pure trigonometric ones.

Further studies need to be performed for different case studies and types of FG sandwich beams, for example, exponentially graded beams.

Acknowledgment

This work has been performed due to the opportunity, confidence and special support of the following Persons: Carlos Heeren, Alberto Bejarano and Gustavo Kato.

Appendix A

Definition of Matrices of type, $\overline{M}_v^{a,b}$

The matrices associated with the terms in the generalized bending governing equations (Eq. (10a-e)) are the following:

$$\overline{M}^{0,0} = \begin{bmatrix} -\alpha & 0 & 0 & 0 \\ 0 & 0 & 0 & 0 \\ 0 & y^*\alpha & 0 & q^*\alpha \end{bmatrix}, \quad \overline{M}^{0,1} = \begin{bmatrix} 0 & -y^{**}\alpha^2 & \alpha^2 & -q^*\alpha^2 \\ 0 & 0 & 0 & 0 \\ 0 & 0 & 0 & 0 \end{bmatrix},$$

$$\overline{M}^{0,2} = \begin{bmatrix} 0 & -\alpha^2 & 0 & 0 \\ 0 & 0 & 0 & 0 \\ 0 & 0 & 0 & 0 \end{bmatrix}, \quad \overline{M}^{0,3} = \begin{bmatrix} 0 & 0 & 0 & 0 \\ 0 & 0 & 0 & 0 \\ 0 & 0 & 0 & \alpha \end{bmatrix},$$

$$\overline{M}^{0,4} = \begin{bmatrix} 0 & 0 & 0 & 0 \\ 0 & 0 & 0 & 0 \\ 0 & \alpha & 0 & 0 \end{bmatrix}, \quad \overline{M}^{0,5} = \begin{bmatrix} 0 & 0 & 0 & 0 \\ 0 & 0 & 0 & 1 \\ 0 & 0 & 0 & 0 \end{bmatrix},$$

$$\overline{M}_x^{1,0} = \begin{bmatrix} -\alpha^2 & 0 & 0 & 0 \\ 0 & 0 & 0 & 0 \\ 0 & -y^*\alpha^2 & 0 & -q^*\alpha^2 \end{bmatrix}, \quad \overline{M}_x^{1,1} = \begin{bmatrix} 0 & -y^{**}\alpha^3 & \alpha^3 & -q^*\alpha^3 \\ 0 & 0 & 0 & 0 \\ 0 & 0 & 0 & 0 \end{bmatrix},$$

$$\overline{M}_x^{1,2} = \begin{bmatrix} 0 & -\alpha^3 & 0 & 0 \\ 0 & 0 & 0 & 0 \\ 0 & 0 & 0 & 0 \end{bmatrix}, \quad \overline{M}_x^{1,3} = \begin{bmatrix} 0 & 0 & 0 & 0 \\ 0 & 0 & 0 & 0 \\ 0 & 0 & 0 & -\alpha^2 \end{bmatrix},$$

$$\overline{M}_x^{1,4} = \begin{bmatrix} 0 & 0 & 0 & 0 \\ 0 & 0 & 0 & 0 \\ 0 & -\alpha^2 & 0 & 0 \end{bmatrix}, \quad \overline{M}_x^{1,5} = \begin{bmatrix} 0 & 0 & 0 & 0 \\ 0 & 0 & 0 & \alpha \\ 0 & 0 & 0 & 0 \end{bmatrix}$$

$$\overline{M}_x^{2,0} = \begin{bmatrix} \alpha^3 & 0 & 0 & 0 \\ 0 & 0 & 0 & 0 \\ 0 & -y^*\alpha^3 & 0 & -q^*\alpha^3 \end{bmatrix}, \quad \overline{M}_x^{2,1} = \begin{bmatrix} 0 & y^{**}\alpha^4 & -\alpha^4 & q^*\alpha^4 \\ 0 & 0 & 0 & 0 \\ 0 & 0 & 0 & 0 \end{bmatrix},$$

$$\overline{M}_x^{2,2} = \begin{bmatrix} 0 & \alpha^4 & 0 & 0 \\ 0 & 0 & 0 & 0 \\ 0 & 0 & 0 & 0 \end{bmatrix}, \quad \overline{M}_x^{2,3} = \begin{bmatrix} 0 & 0 & 0 & 0 \\ 0 & 0 & 0 & 0 \\ 0 & 0 & 0 & -\alpha^3 \end{bmatrix},$$

$$\overline{M}_x^{2,4} = \begin{bmatrix} 0 & 0 & 0 & 0 \\ 0 & 0 & 0 & 0 \\ 0 & -\alpha^3 & 0 & 0 \end{bmatrix}, \quad \overline{M}_x^{2,5} = \begin{bmatrix} 0 & 0 & 0 & 0 \\ 0 & 0 & 0 & -\alpha^2 \\ 0 & 0 & 0 & 0 \end{bmatrix},$$

References

[1] M. B. Bever, P. E. Duwez: Gradients in composite materials. Mater. Sci. Eng. 10 (1972) pp. 1-8.

[2] J.L. Mantari, A.S. Oktem, C. Guedes Soares: Bending response of functionally graded plates by using a new higher order shear deformation theory. Compos. Struct. 94 (2012) pp. 714-723.

[3] J.L. Mantari, C. Guedes Soares: A novel higher-order shear deformation theory with stretching effect for functionally graded plates. Compos. Struct. 94 (2012) pp. 1991-2000.

[4] J.L. Mantari, E.M. Bonilla, C. Guedes Soares. A new tangential-exponential higher order shear deformation theory for advanced composite plates. Composites Part B: Engineering 60 (2014) 319-328.

[5] J.L. Mantari, C. Guedes Soares: Generalized hybrid quasi-3D shear deformation theory for the static analysis of advanced composite plates. Compos. Struct. 94 (2012) 2561-2575. Compos. Struct. 94 (2012) pp. 2561-2575.

[6] J.L. Mantari, C. Guedes Soares: Finite element formulation of a generalized higher order shear deformation theory for advanced composite plates. Compos. Struct. 96 (2013) pp. 545-553.

[7] J.L. Mantari, C. Guedes Soares: Five-unknowns generalized hybrid-type quasi-3D HSDT for advanced composite plates. Appl. Math. Modell. (2015).

[8] K. Swaminathan, D. T. Naveenkumar, A. M. Zenkour, E. Carrera: Stress, vibration and buckling analysis of FGM plates- A state of the art review. Composite Structures 120 (2015) pp. 10-31.

[9] A. M. A. Neves, A. J. M. Ferreira, E. Carrera, M. Cinefra, C. M. C. Roque, R. M. N. Jorge, C. M. M. Soares: Static, free vibration and buckling analysis of isotropic and sandwich functionally graded plates using a quasi-3D higher-order shear deformation theory and a meshless technique. Composites: Part B 44 (2013) pp. 657-674.

[10] E. Carrera, S. Brischetto: Modeling and Analysis of Functionally Graded Beams, Plates and Shells: Part II. Mechanics of Advanced Materials and Structures 18 (2011) pp. 1-2.

[11] A. M. A. Zenkour: A comprehensive analysis of functionally graded sandwich plates: Part 1 - deflection and stresses. Int J Solids Struct 42(18-19) (2005) pp 5224-5242.

[12] A. M. A. Zenkour: A comprehensive analysis of functionally graded sandwich plates: Part 2 - buckling and free vibration. Int J Solids Struct 42(18-19) (2005) pp 5243-5258.

[13] A. M. A. Neves, A. J. M. Ferreira, E. Carrera, M. Cinefra, C. M. C. Roque, R. M. N. Jorge, C. M. M. Soares: Free vibration analysis of functionally graded shells by a higher-order shear deformation theory and radial basis functions collocation, accounting for through-the-thickness deformations. European Journal of Mechanics A/Solids 37 (2013) pp. 24-34.

[14] F. A. Fazzolari, E. Carrera: Refined hierarchical kinematics quasi-3D Ritz models for free vibration analysis of doubly curved FGM shells and sandwich shells with FGM core: Journal of Sound and Vibration 333 (2014) pp. 1485-1508.

[15] G. Giunta, S. Belouettar, E. Carrera: Analysis of FGM Beams by Means of Classical and Advanced Theories. Mechanics of Advanced Materials and Structures 17 (2010) pp. 622-635.

[16] G. Giunta, D. Crisafulli, S. Belouettar, E. Carrera: Hierarchical theories for the free vibration analysis of functionally graded beams. Composite Structures 94 (2011) pp. 68-74.

[17] G. Giunta, D. Crisafulli, S. Belouettar, E. Carrera: A thermo-mechanical analysis of functionally graded beams via hierarchical modelling. Composite Structures 95 (2013) pp. 676-690.

[18] Carrera E., Brischetto S., Cinefra M., Soave M.. "Effects of thickness stretching in functionally graded plates and shells", Composites: Part B (2011), 42, pp. 123-130.

[19] Thuc P. Vo, Huu-Tai Thai, Trung-Kien Nguyen, Fawad Inam, Jaehong Lee: Static behaviour of functionally graded sandwich beams using a quasi-3D theory. Composites: Part B 68 (2015) pp 59-74.

[20] M. Filippi M., E. Carrera, A. M. Zenkour: Static analyses of FGM beams by various theories and finite elements. Composites: Part B 72 (2015) pp. 1-9.

[21] J. N. Reddy, C.F. Liu: A higher-order shear deformation theory of laminated elastic shells. Int. J. Eng. Sci. 23 (1985) 319-330.

[22] J. N. Reddy: Mechanics of Laminated Composite Plates: Theory and Analysis, 2nd ed.. CRC Press, Boca Raton (FL), 2004.

Tables caption

Table 1: Shear strain shape functions.

Table 2: Comparison of the maximum vertical displacement of FG S-S beams (Type A).

Table 3: Comparison of the axial stress $\bar{\sigma}_{xx}(a/2, h/2)$ of FG S-S beams (Type A).

Table 4: Comparison of the normal stress $\bar{\sigma}_{zz}(a/2, h/2)$ of FG S-S beams (Type A).

Table 5: Comparison of the shear stress $\bar{\sigma}_{xz}(0,0)$ of FG S-S beams (Type A).

Table 6: The maximum vertical displacement of (1-8-1) FG sandwich beams (Type B).

Table 7: Comparison of the axial stress $\bar{\sigma}_{xx}$ of (1-8-1) FG sandwich S-S beams (Type B).

Table 8: Comparison of the normal stress $\bar{\sigma}_{zz}(a/2, h/2)$ of (1-8-1) FG sandwich S-S beams (Type B).

Table 9: Comparison of the shear stress $\bar{\sigma}_{xz}(0,0)$ of (1-8-1) FG sandwich S-S beams (Type B).

Table 10: The maximum vertical displacement of FG sandwich S-S beams (Type C).

Table 11: Comparison of the axial stress $\bar{\sigma}_{xx}$ of FG sandwich S-S beams (Type C).

Table 12: Comparison of the normal stress $\bar{\sigma}_{zz}$ of FG sandwich S-S beams (Type C).

Table 13: Comparison of the shear stress $\bar{\sigma}_{xz}$ of FG sandwich S-S beams (Type C).

Figures caption

Figure 1. Geometry and coordinate of a FG sandwich beam.

Figure 2. Comparison of the shear stress through the thickness of FG S-S beams under uniform load (Type A, $a/h = 5$).

Figure 3: Variation of the stresses through the thickness of (1-8-1) FG sandwich S-S beams under uniform load (HSDT4, Type B, $a/h = 5$).

Figure 4: Variation of the vertical displacement through the thickness of FG sandwich S-S beams under uniform load (HSDT1, Type C, $a/h = 5$).

Figure 5: Variation of the axial stress through the thickness of FG sandwich S-S beams under uniform load (HSDT4, Type C, $a/h = 5$).

Figure 6: Variation of the normal stress through the thickness of FG sandwich S-S beams under uniform load (HSDT4, Type C, $a/h = 5$).

Figure 7: Variation of the shear stress through the thickness of FG sandwich S-S beams under uniform load (HSDT4, Type C, $a/h = 5$).

Tables

Table 1.

Model	function $f(z)$ and $g(z)$	
Polynomial HSDT1	$f(z)=\frac{4z^3}{3h^2}$	$g(z)=1-\frac{4z^2}{h^2}$
Trigonometric HSDT2	$f(z)=4sin(\frac{z}{4})$	$g(z)=cos(\frac{z}{4})$
Trigonometric HSDT3	$f(z)=tan(\frac{z}{4h})$	$g(z)=cos(\frac{z}{4h})$
Hybrid HSDT4	$f(z)=tan(\frac{z}{4h})$	$g(z)=1-\frac{4z^2}{h^2}$

Table 2.

a/h	Theory	$p=0$	$p=1$	$p=2$	$p=5$	$p=10$
5	Vo et al.	3.1397	6.1338	7.8606	9.6037	10.7578
	HSDT1	3.1397	6.1338	7.8606	9.6037	10.7578
	HSDT2	3.1397	6.1338	7.8606	9.6037	10.7577
	HSDT3	3.1397	6.1338	7.8605	9.6033	10.7575
	HSDT4	3.1397	6.1338	7.8605	9.6033	10.7575
20	Vo et al.	2.8947	5.7201	7.2805	8.6479	9.5749
	HSDT1	2.8947	5.7201	7.2805	8.6479	9.5748
	HSDT2	2.8947	5.7201	7.2805	8.6479	9.5748
	HSDT3	2.8947	5.7201	7.2805	8.6479	9.5749
	HSDT4	2.8947	5.7201	7.2805	8.6479	9.5748

Table 3.

a/h	Theory	$p = 0$	$p = 1$	$p = 2$	$p = 5$	$p = 10$
5	Vo et al.	3.8005	5.8812	6.8818	8.1140	9.7164
	HSDT1	3.8005	5.8812	6.8819	8.1140	9.7164
	HSDT2	3.8006	5.8812	6.8819	8.1140	9.7165
	HSDT3	3.8007	5.8815	6.8822	8.1141	9.7166
	HSDT4	3.8004	5.8810	6.8815	8.1135	9.7159
20	Vo et al.	15.0125	23.2046	27.0988	31.8137	38.1395
	HSDT1	15.0126	23.2047	27.0990	31.8139	38.1393
	HSDT2	15.0126	23.2047	27.0990	31.8139	38.1402
	HSDT3	15.0141	23.2073	27.1017	31.8168	38.1429
	HSDT4	15.0126	23.2047	27.0989	31.8138	38.1395

Table 4.

a/h	Theory	$p = 0$	$p = 1$	$p = 2$	$p = 5$	$p = 10$
	Vo et al.	0.1352	0.0670	0.0925	0.0180	-0.0181
	HSDT1	0.1352	0.0670	0.0925	0.0181	-0.0181
	HSDT2	0.1352	0.0671	0.0926	0.0182	-0.0180
	HSDT3	0.1363	0.0689	0.0946	0.0202	-0.0157
	HSDT4	0.1351	0.0670	0.0924	0.0178	-0.0183
20	Vo et al.	0.0337	-0.5880	-0.6269	-1.1698	-1.5572
	HSDT1	0.0338	-0.5879	-0.6269	-1.1697	-1.5571
	HSDT2	0.0338	-0.5879	-0.6268	-1.1686	-1.5543
	HSDT3	0.0389	-0.5793	-0.6173	-1.1594	-1.5458
	HSDT4	0.0338	-0.5879	-0.6269	-1.1697	-1.5571

Table 5.

a/h	Theory	$p = 0$	$p = 1$	$p = 2$	$p = 5$	$p = 10$
	Vo et al.	0.7233	0.7233	0.6622	0.5840	0.6396
	HSDT1	0.7233	0.7233	0.6622	0.5840	0.6396
	HSDT2	0.7232	0.7232	0.6622	0.5840	0.6396
	HSDT3	0.7223	0.7223	0.6612	0.5829	0.6385
	HSDT4	0.7223	0.7223	0.6612	0.5829	0.6385
20	Vo et al.	0.7432	0.7432	0.6809	0.6010	0.6583
	HSDT1	0.7433	0.7433	0.6809	0.6011	0.6584
	HSDT2	0.7433	0.7433	0.6809	0.6011	0.6584
	HSDT3	0.7423	0.7424	0.6799	0.6005	0.6522
	HSDT4	0.7423	0.7423	0.6799	0.6005	0.6522

Table 6.

a/h	Theory	$p = 0$	$p = 1$	$p = 2$	$p = 5$	$p = 10$
5	Vo et al.	3.9374	6.5505	7.7721	8.8089	9.2426
	HSDT1	3.9374	6.5505	7.7721	8.8089	9.2426
	HSDT2	3.9374	6.5505	7.7721	8.8089	9.2426
	HSDT3	3.9374	6.5505	7.7719	8.8081	9.2417
	HSDT4	3.9373	6.5505	7.7719	8.8081	9.2417
20	Vo et al.	3.6841	6.1383	7.2143	7.9435	8.1710
	HSDT1	3.6841	6.1383	7.2143	7.9435	8.1709
	HSDT2	3.6841	6.1383	7.2142	7.9435	8.1710
	HSDT3	3.6841	6.1383	7.2142	7.9435	8.1709
	HSDT4	3.6841	6.1383	7.2143	7.9435	8.1709

Table 7.

a/h	Theory	$p = 0$	$p = 1$	$p = 2$	$p = 5$	$p = 10$
5	Vo et al.	4.4603	6.0069	6.5253	6.8927	7.2292
	HSDT1	4.4604	6.0069	6.5254	6.8928	7.2293
	HSDT2	4.4604	6.0070	6.5254	6.8928	7.2293
	HSDT3	4.4607	6.0073	6.5256	6.8928	7.2292
	HSDT4	4.4602	6.0067	6.5250	6.8922	7.2286
20	Vo et al.	17.6318	23.7073	25.6848	26.9703	28.2298
	HSDT1	17.6319	23.7074	25.6849	26.9705	28.2299
	HSDT2	17.6319	23.7074	25.6849	26.9706	28.2301
	HSDT3	17.6340	23.7100	25.6875	26.9730	28.2324
	HSDT4	17.6319	23.7074	25.6848	26.9703	28.2298

Table 8.

a/h	Theory	$p = 0$	$p = 1$	$p = 2$	$p = 5$	$p = 10$
5	Vo et al.	0.0872	0.1043	0.1277	0.0619	-0.0001
	HSDT1	0.0873	0.1044	0.1277	0.0620	-0.0001
	HSDT2	0.0873	0.1044	0.1278	0.0621	0.0002
	HSDT3	0.0888	0.1063	0.1296	0.0638	0.0017
	HSDT4	0.0872	0.1043	0.1276	0.0617	-0.0004
20	Vo et al.	-0.2904	-0.4373	-0.4179	-0.8042	-1.1450
	HSDT1	-0.2903	-0.4372	-0.4178	-0.8042	-1.1449
	HSDT2	-0.2903	-0.4372	-0.4177	-0.8043	-1.1442
	HSDT3	-0.2832	-0.4285	-0.4087	-0.7953	-1.1363
	HSDT4	-0.2903	-0.4372	-0.4178	-0.8042	-1.1449

Table 9.

a/h	Theory	$p=0$	$p=1$	$p=2$	$p=5$	$p=10$
5	Vo et al.	0.7486	0.7219	0.6365	0.5262	0.5733
	HSDT1	0.7486	0.7219	0.6365	0.5262	0.5733
	HSDT2	0.7486	0.7219	0.6365	0.5262	0.5733
	HSDT3	0.7476	0.7209	0.6354	0.5249	0.5720
	HSDT4	0.7476	0.7209	0.6354	0.5249	0.5720
20	Vo et al.	0.7683	0.7418	0.6543	0.5414	0.5900
	HSDT1	0.7684	0.7419	0.6544	0.5415	0.5900
	HSDT2	0.7684	0.7419	0.6544	0.5415	0.5900
	HSDT3	0.7674	0.7409	0.6533	0.5401	0.5861
	HSDT4	0.7673	0.7409	0.6533	0.5401	0.5861

Table 10.

p	Theory	*a*/*h* = 5		*a*/*h* = 20	
		1-2-1	2-2-1	1-2-1	2-2-1
0	Vo et al.	3.1397	3.1397	2.8947	2.8947
	HSDT1	3.1397	3.1397	2.8947	2.8947
	HSDT2	3.1397	3.1397	2.8947	2.8947
	HSDT3	3.1397	3.1397	2.8947	2.8947
	HSDT4	3.1397	3.1397	2.8947	2.8947
1	Vo et al.	5.3612	5.7777	5.0975	5.5040
	HSDT1	5.3611	5.7777	5.0975	5.5040
	HSDT2	5.3611	5.7777	5.0975	5.5040
	HSDT3	5.3611	5.7777	5.0975	5.5040
	HSDT4	5.3611	5.7777	5.0975	5.5040
2	Vo et al.	6.6913	7.4629	6.4235	7.1790
	HSDT1	6.6913	7.4630	6.4235	7.1791
	HSDT2	6.6913	7.4630	6.4235	7.1791
	HSDT3	6.6913	7.4631	6.4235	7.1791
	HSDT4	6.6913	7.4630	6.4235	7.1791
5	Vo et al.	8.4276	9.6459	8.1589	9.3498
	HSDT1	8.4276	9.6462	8.1589	9.3501
	HSDT2	8.4276	9.6462	8.1589	9.3501
	HSDT3	8.4277	9.6463	8.1589	9.3500
	HSDT4	8.4276	9.6463	8.1589	9.3501
10	Vo et al.	9.3099	10.6769	9.0413	10.3715
	HSDT1	9.3099	10.6772	9.0413	10.3719
	HSDT2	9.3099	10.6772	9.0413	10.3719
	HSDT3	9.3100	10.6773	9.0413	10.3718
	HSDT4	9.3099	10.6773	9.0413	10.3719

Table 11.

p	Theory	*a*/*h* = 5		*a*/*h* = 20	
		1-2-1	2-2-1	1-2-1	2-2-1
0	Vo et al.	3.8005	3.8005	15.0125	15.0125
	HSDT1	3.8005	3.8005	15.0126	15.0126
	HSDT2	3.8006	3.8006	15.0126	15.0126
	HSDT3	3.8007	3.8007	15.0141	15.0141
	HSDT4	3.8004	3.8004	15.0126	15.0126
1	Vo et al.	1.2315	1.2459	4.8797	4.9360
	HSDT1	1.2315	1.2459	4.8797	4.9360
	HSDT2	1.2315	1.2459	4.8797	4.9360
	HSDT3	1.2316	1.2460	4.8803	4.9367
	HSDT4	1.2314	1.2459	4.8797	4.9360
2	Vo et al.	1.5505	1.5849	6.1526	6.2882
	HSDT1	1.5505	1.5850	6.1526	6.2883
	HSDT2	1.5505	1.5850	6.1526	6.2883
	HSDT3	1.5506	1.5851	6.1535	6.2892
	HSDT4	1.5504	1.5849	6.1526	6.2883
5	Vo et al.	1.9672	2.0160	7.8185	8.0100
	HSDT1	1.9672	2.0160	7.8186	8.0100
	HSDT2	1.9672	2.0160	7.8186	8.0100
	HSDT3	1.9674	2.0162	7.8197	8.0112
	HSDT4	1.9672	2.0160	7.8186	8.0100
10	Vo et al.	2.1788	2.2161	8.6655	8.8094
	HSDT1	2.1788	2.2162	8.6656	8.8095
	HSDT2	2.1788	2.2162	8.6656	8.8095
	HSDT3	2.1791	2.2164	8.6669	8.8430
	HSDT4	2.1788	2.2161	8.6656	8.8418

Table 12.

p	Theory	$a/h = 5$		$a/h = 20$	
		1-2-1	2-2-1	1-2-1	2-2-1
0	Vo et al.	0.1352	0.1352	0.0337	0.0337
	HSDT1	0.1352	0.1352	0.0338	0.0338
	HSDT2	0.1352	0.1352	0.0338	0.0338
	HSDT3	0.1363	0.1363	0.0389	0.0389
	HSDT4	0.1351	0.1351	0.0338	0.0338
1	Vo et al.	0.0447	0.0286	0.0111	-0.0625
	HSDT1	0.0447	0.0286	0.0112	-0.0625
	HSDT2	0.0447	0.0287	0.0112	-0.0625
	HSDT3	0.0451	0.0291	0.0133	-0.0602
	HSDT4	0.0447	0.0286	0.0112	-0.0625
2	Vo et al.	0.0564	0.0341	0.0141	-0.0895
	HSDT1	0.0564	0.0341	0.0141	-0.0895
	HSDT2	0.0564	0.0342	0.0141	-0.0895
	HSDT3	0.0570	0.0348	0.0170	-0.0864
	HSDT4	0.0564	0.0341	0.0141	-0.0895
5	Vo et al.	0.0712	0.0454	0.0178	-0.1010
	HSDT1	0.0712	0.0455	0.0178	-0.1009
	HSDT2	0.0712	0.0455	0.0178	-0.1009
	HSDT3	0.0720	0.0463	0.0216	-0.0969
	HSDT4	0.0712	0.0455	0.0178	-0.1009
10	Vo et al.	0.0783	0.0518	0.0195	-0.0998
	HSDT1	0.0783	0.0518	0.0196	-0.0997
	HSDT2	0.0784	0.0518	0.0196	-0.0997
	HSDT3	0.0792	0.0528	0.0238	-0.0737
	HSDT4	0.0783	0.0518	0.0196	-0.0780

Table 13.

p	Theory	*a*/*h* = 5		*a*/*h* = 20	
		1-2-1	2-2-1	1-2-1	2-2-1
0	Vo et al.	0.7233	0.7233	0.7432	0.7432
	HSDT1	0.7233	0.7233	0.7433	0.7433
	HSDT2	0.7233	0.7233	0.7433	0.7433
	HSDT3	0.7223	0.7223	0.7423	0.7423
	HSDT4	0.7223	0.7223	0.0338	0.7423
1	Vo et al.	0.7993	0.8342	0.8193	0.7432
	HSDT1	0.7993	0.8342	0.8194	0.8553
	HSDT2	0.7993	0.8343	0.8194	0.8553
	HSDT3	0.7983	0.8333	0.8185	0.8544
	HSDT4	0.7983	0.8333	0.0112	0.8544
2	Vo et al.	0.8349	0.8920	0.8556	0.9142
	HSDT1	0.8349	0.8920	0.8557	0.9143
	HSDT2	0.8349	0.8920	0.8557	0.9143
	HSDT3	0.8340	0.8911	0.8549	0.9135
	HSDT4	0.8340	0.8911	0.0141	0.9135
5	Vo et al.	0.8763	0.9683	0.8986	0.9927
	HSDT1	0.8763	0.9683	0.8987	0.9928
	HSDT2	0.8763	0.9683	0.8987	0.9928
	HSDT3	0.8754	0.9676	0.8975	0.9900
	HSDT4	0.8754	0.9676	0.0178	0.9900
10	Vo et al.	0.8980	1.0148	0.9214	1.0405
	HSDT1	0.8980	1.0148	0.9214	1.0406
	HSDT2	0.8980	1.0148	0.9214	1.0406
	HSDT3	0.8972	1.0140	0.9227	1.0396
	HSDT4	0.8972	1.0140	0.0196	1.0396

Figures

Figure 1.

(a) Type A

(b) Type B

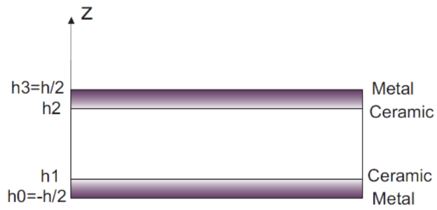

(a) Type C

Figure 2.

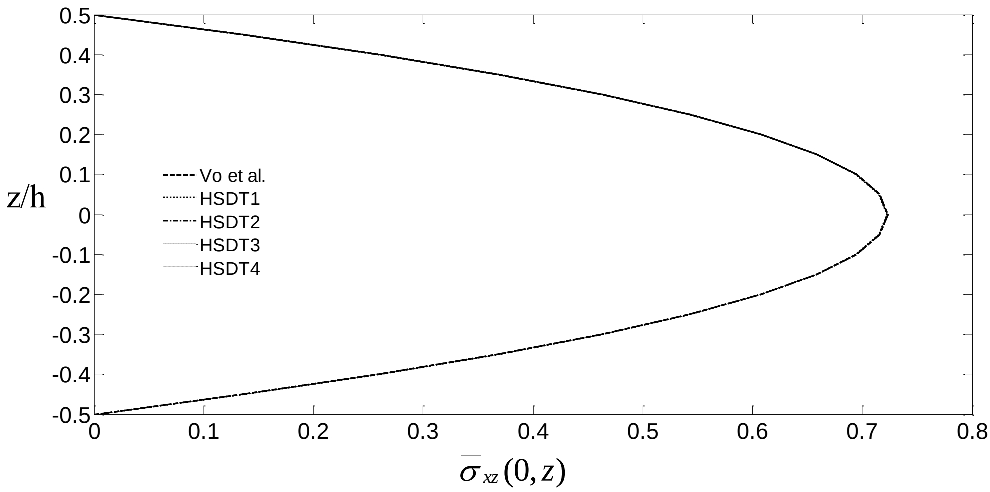

(a) p = 0

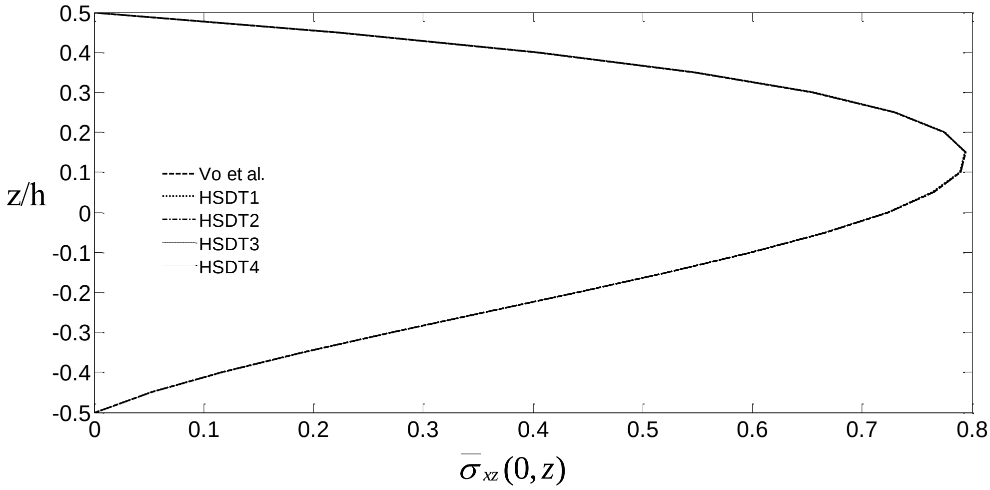
z/h
Vo et al.
HSDT1
HSDT2
HSDT3
HSDT4
$\bar{\sigma}_{xz}(0,z)$

(b) p = 1

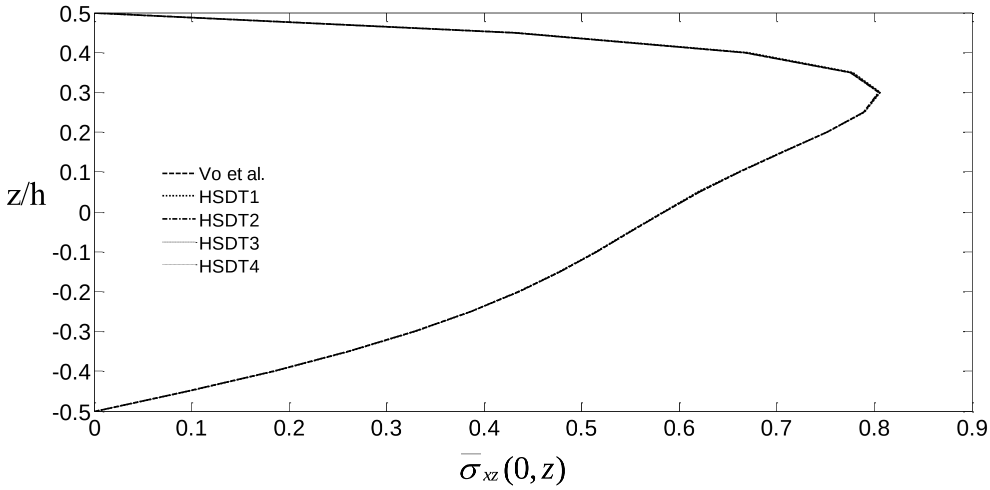
z/h
Vo et al.
HSDT1
HSDT2
HSDT3
HSDT4
$\bar{\sigma}_{xz}(0,z)$

(c) p = 5

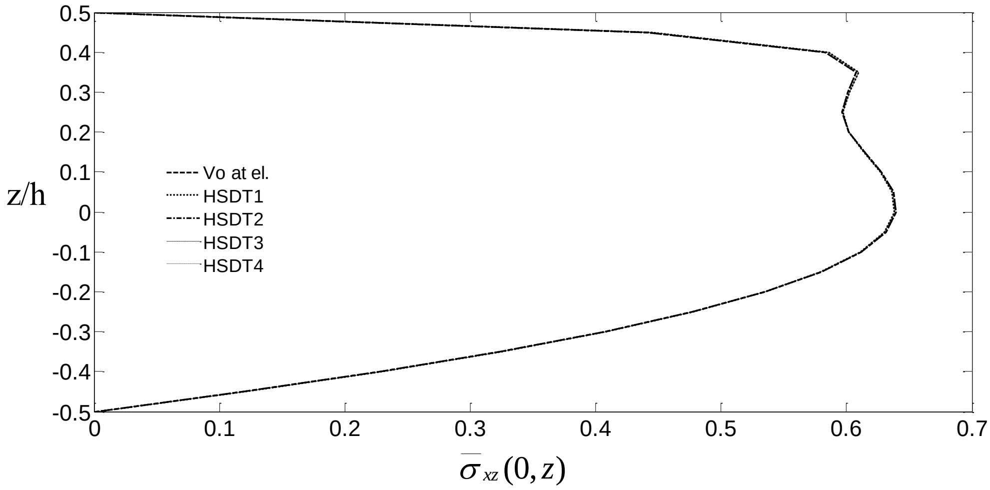
z/h
Vo at el.
HSDT1
HSDT2
HSDT3
HSDT4
$\bar{\sigma}_{xz}(0,z)$

(d) p = 10

Figure 3.

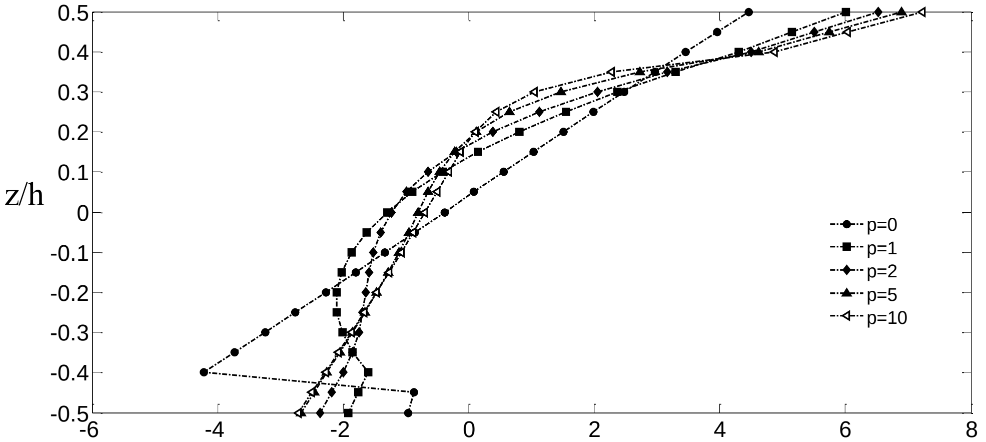

$\bar{\sigma}_{xx}(a/2,z)$

(a) Axial stress

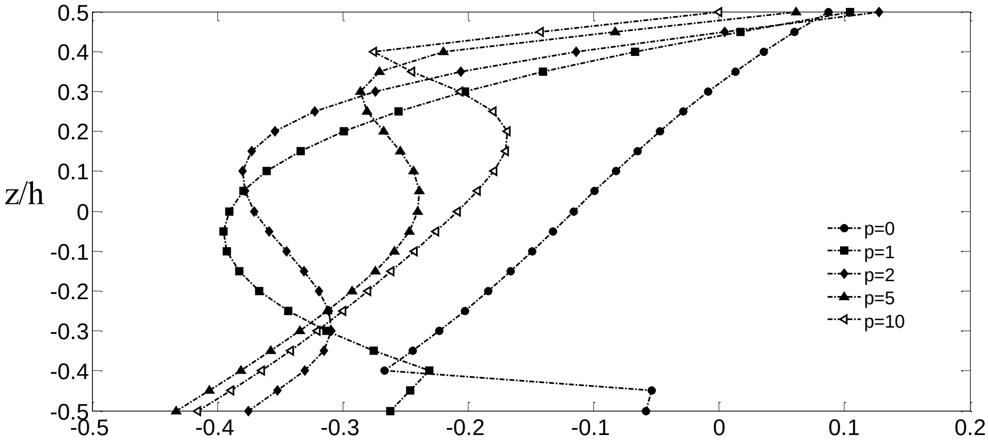

$\bar{\sigma}_{zz}(a/2,z)$

(b) Normal stress

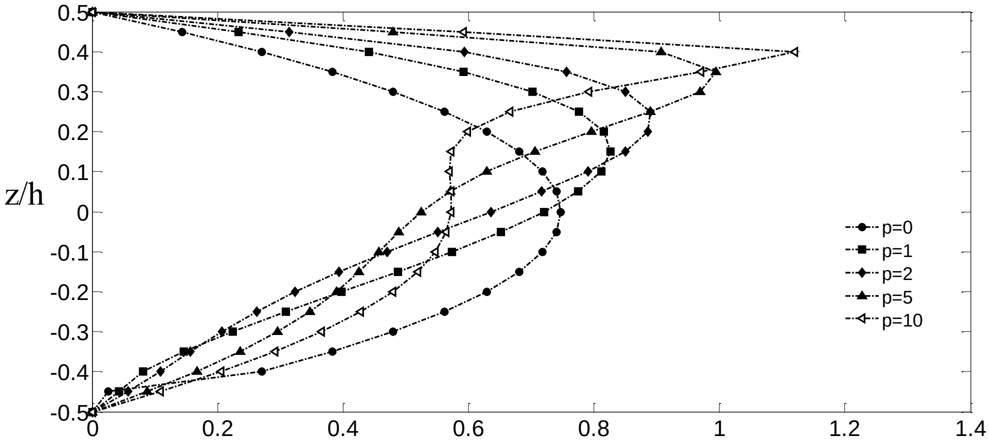

$\bar{\sigma}_{xz}(0,z)$

(c) Shear stress

Figure 4.

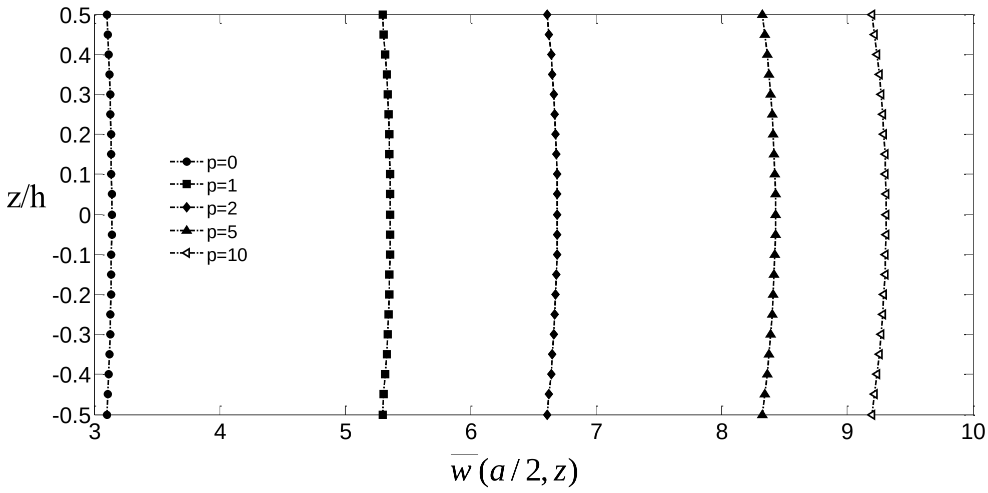

(a) (1-2-1)

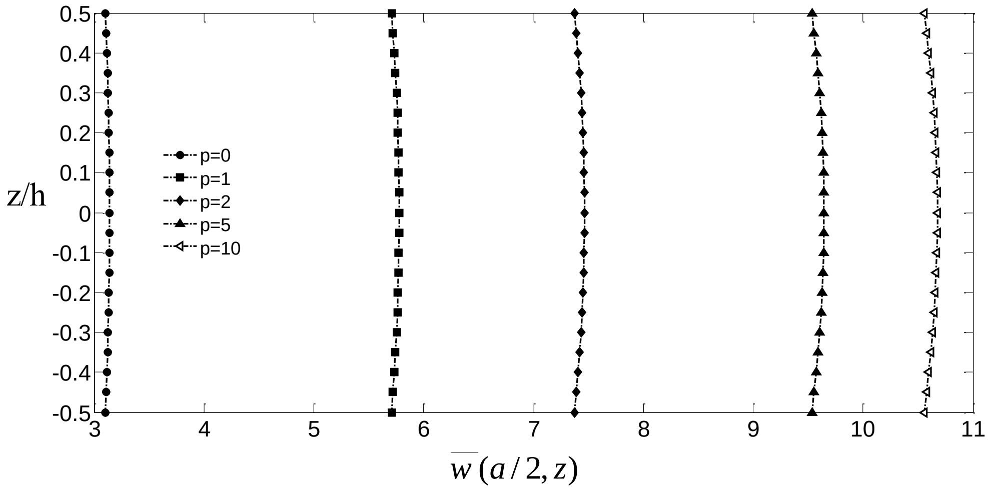

(b) (2-2-1)

Figure 5.

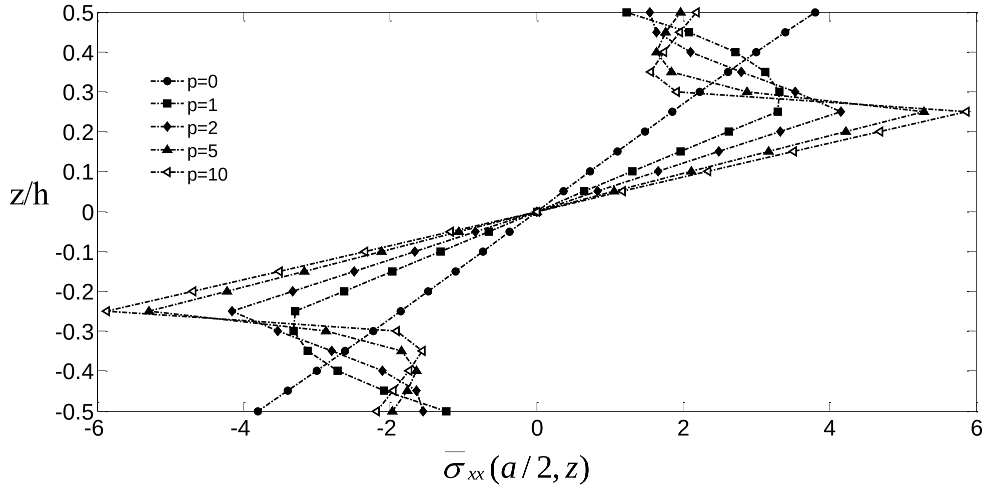

(a) (1-2-1)

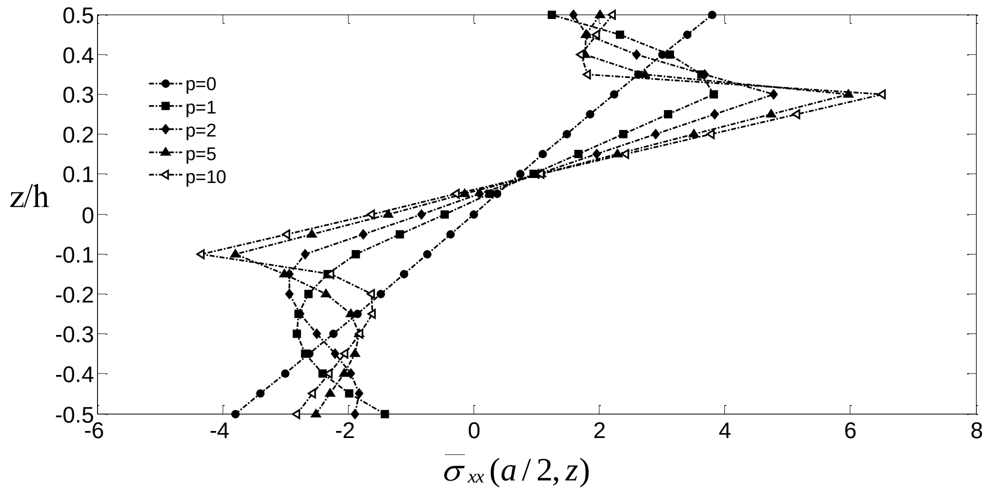

(b) (2-2-1)

Figure 6.

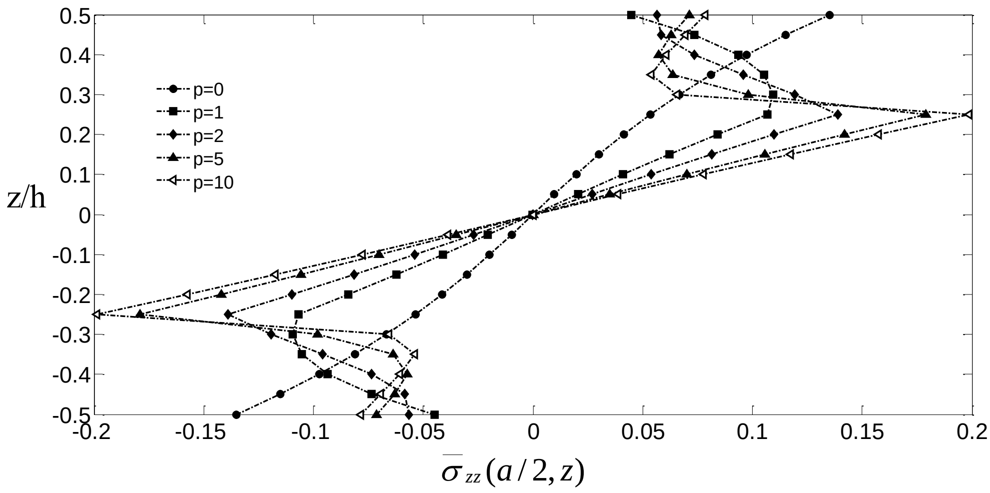

(a) (1-2-1)

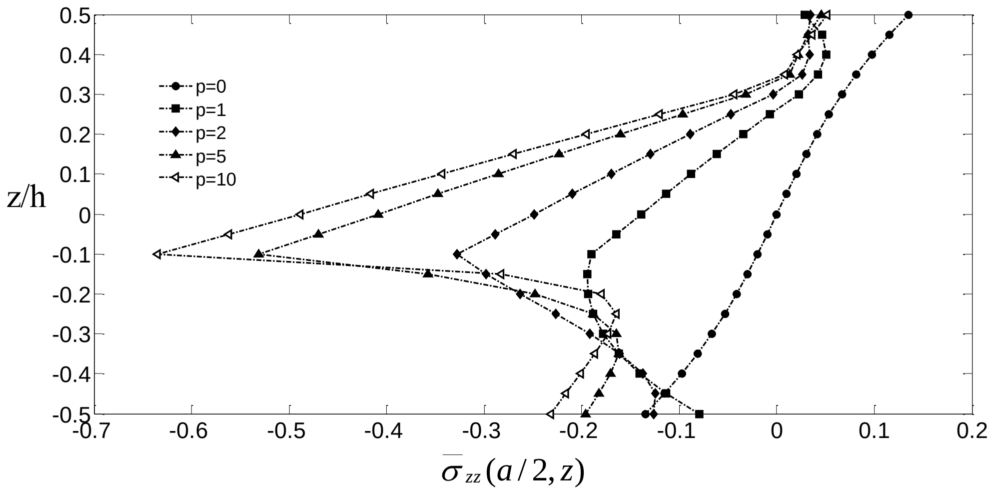

(b) (2-2-1)

Figure 7.

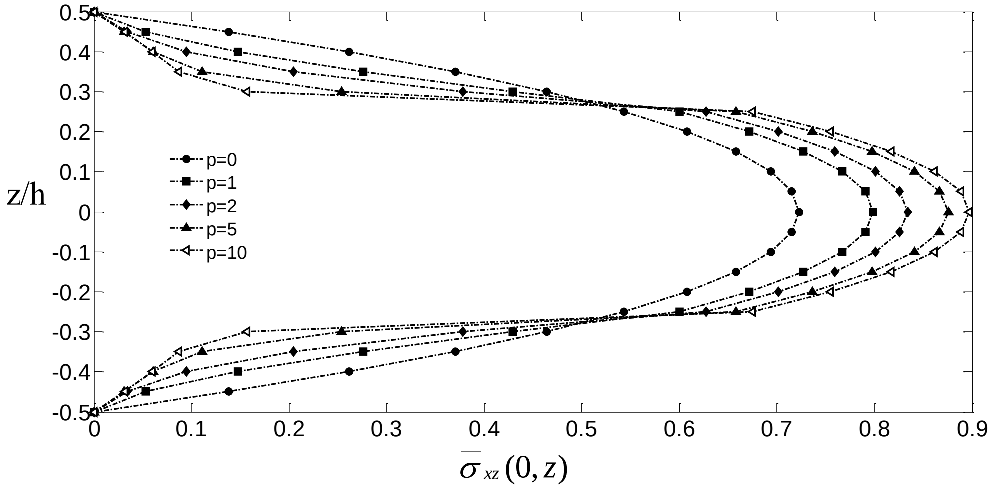

(a) (1-2-1)

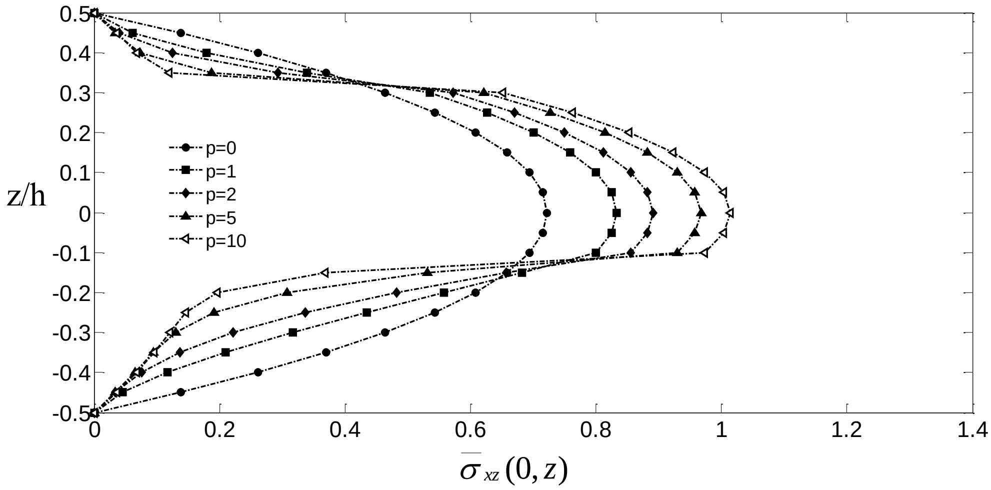

(b) (2-2-1)